Pergamon

Geothermics, Vol. 23, No. 1, pp. 3–20, 1994
CNR
Elsevier Science Ltd
Printed in Great Britain
0375-6505/94 $7.00+0.00

0375-6505(93)E0006-J

MODELING STUDIES OF HEAT TRANSFER AND PHASE DISTRIBUTION IN TWO-PHASE GEOTHERMAL RESERVOIRS

C. H. LAI,* G. S. BODVARSSON* and A. H. TRUESDELL†

**Earth Sciences Division, Lawrence Berkeley Laboratory, Berkeley, CA 94720, U.S.A. and*
†*Consultant, Menlo Park, CA 94025, U.S.A.*

(*Received February* 1993; *accepted for publication August* 1993)

Abstract—Phase distribution as well as mass flow and heat transfer behavior in two-phase geothermal systems have been studied by numerical modeling. A two-dimensional porous-slab model was used with a non-uniform heat flux boundary condition at the bottom. Steady-state solutions are obtained for the phase distribution and heat transfer behavior for cases with different mass of fluid (gas saturation) in place, permeabilities, and capillary pressures. The results obtained show very efficient heat transfer in the vapor-dominated zone due to the development of heat pipes and near-uniform saturations. The phase distribution below the vapor-dominated zone depends on permeability. For relatively high-permeability systems, single-phase liquid zones prevail, with convection providing the energy throughput. For lower permeability systems, a two-phase liquid-dominated zone develops, because single-phase liquid convection is not sufficient to dissipate heat released from the source. These results are consistent with observations from the field, where most high-temperature liquid-dominated two-phase systems have relatively low permeabilities (e.g. Krafla, Iceland; Olkaria, Kenya; Baca, New Mexico). The numerical results obtained also show that for high heat flow a high-temperature single-phase vapor zone can develop below a typical (240°C) vapor-dominated zone, as has recently been found at The Geysers, California, and Larderello, Italy.

Key words: geothermal reservoirs, two-phase geothermal systems, modeling.

INTRODUCTION

Large two-phase vapor-dominated geothermal reservoirs have been exploited at The Geysers, California; Larderello, Italy; and Kamojang, Indonesia. These reservoirs produce only steam, and have nearly vapor-static pressure gradients at corresponding saturation temperatures. Although long exploited (Larderello from 1904), these reservoirs are not fully understood. White *et al.* (1971) proposed a model involving counterflow of ascending steam and descending condensate, which has become generally accepted and was successfully simulated by Pruess (1985), and Ingebritsen and Sorey (1988). In this model boiling at a deep brine "water table" was assumed, with steam moving upward in large fractures and condensing at the top of the reservoir. This condensate flowed downward by gravity through the rock matrix and small fractures to replenish the brine. Support for the existence of deep liquid saturation (boiling brine) at Larderello comes from temperatures in deep drillholes that in part agree with those expected in a boiling water column beneath a 2700 m deep water table (Pruess *et al.*, 1987).

The model did not explain all the features of vapor-dominated reservoirs. Lateral variations in steam chemistry at Larderello were explained by D'Amore and Truesdell (1979) as due to open-system (Rayleigh-type) condensation of steam flowing laterally from central upflow zones and with resulting condensate flowing back to the center within the underlying water table. Support for this model comes from inward sloping water tables found in non-productive zones at the edges of Larderello and The Geysers (Calore *et al.*, 1980; Enedy *et al.*, 1990). These marginal water tables also support the assumed existence of a deep boiling brine.

However, recent discoveries in the northern part of The Geysers and some evidence from Larderello suggest that dry, high-temperature rock underlies the vapor-dominated reservoir. Drenick (1986) and Walters *et al.* (1988) described some wells in the Coldwater Creek field of The Geysers as entering a high-temperature zone (up to 347°C) only 200 m below a normal 245°C vapor-dominated reservoir. At Larderello a number of deep wells showed temperatures above 350°C and although some of these may be related to deep liquid (Pruess *et al.*, 1987), well San Pompeo 2 encountered a superheated vapor zone with temperature of 394°C at a depth of 2650 m (Cappetti *et al.*, 1985). A conceptual model for the origin of these high-temperature zones as relics of hot rock not yet cooled by downward expanding vapor-dominated reservoirs was suggested by Truesdell (1991). In this model high-temperature rock replaces the boiling liquid, and condensate entering the hot rock evaporates and flows directly upwards. These observations indicate that a boiling deep liquid is not necessary to support a vapor-dominated reservoir. There are numerous studies that support this observation.

Experimental and analytical studies of boiling in liquid-saturated porous layers of finite lateral extent with heating from below and cooling from above have been conducted by many investigators (Lee and Nilson, 1977; Sondergeld and Turcotte, 1977; Schubert and Straus, 1980; Bau and Torrance, 1982; Torrance, 1983; and Ramesh and Torrance, 1990). These studies show that two distinct zones are observed in the porous layer. The upper zone is liquid water and the lower zone is a two-phase mixture of vapor and water at the boiling temperature. Vapor is produced at the bottom heating surface and rises to the top of the two-phase zone, where it condenses to liquid and releases its latent heat. The condensate percolates down to the bottom surface where it is heated and evaporated again. This process forms the boiling cycle, usually referred to as heat pipe. When the applied heat flux at the bottom surface exceeds a critical value, the lower two-phase zone may disappear and be replaced by a dry vapor zone.

In the above studies no deep liquid zone underlying the vapor-dominated zone was found. Some of the experimental results resembled the north Geysers with dry, elevated temperatures at the bottom whenever heat flux was high enough. In contrast, numerical simulations performed by Pruess (1985) and Ingebritsen and Sorey (1988) found a boiling two-phase liquid (liquid-dominated) layer below the vapor-dominated zone.

The objectives of the present study are (1) to characterize behavior of flow and heat transfer processes in vapor-dominated geothermal reservoirs, and (2) to explain the thermodynamic conditions encountered in the high-temperature reservoirs observed in The Geysers and Larderello.

DESCRIPTION OF THE PROBLEM

A numerical study of steady-state two-phase geothermal reservoirs was performed using a two-dimensional porous-slab model with all boundaries impermeable to fluid flow. The porous slab is assumed to have non-uniform heat flux distribution at the bottom, reflecting situations where a localized magma body is found below the reservoir. Figure 1 shows a schematic representation of the right half of the physical problem considered in the study; half of the reservoir is adequate because we assume the problem to be symmetric with respect to the vertical axis at $x = 0$. Physical dimensions of the half slab are 2000 and 1500 m in width and thickness, respectively. A constant heat flux boundary condition is imposed over a 500 m length in the left bottom surface of the model. Constant heat flux rather than constant temperature was chosen, because field data have shown a near constant heat flux over large areas of many two-phase geothermal fields. The heat flux is chosen to be 2 W/m^2 mainly on the basis of field measurements (Thomas, 1986; Walters and Combs, 1989). The remaining bottom surface and the vertical walls of the slab are closed to heat flow. The slab is overlain by an impermeable

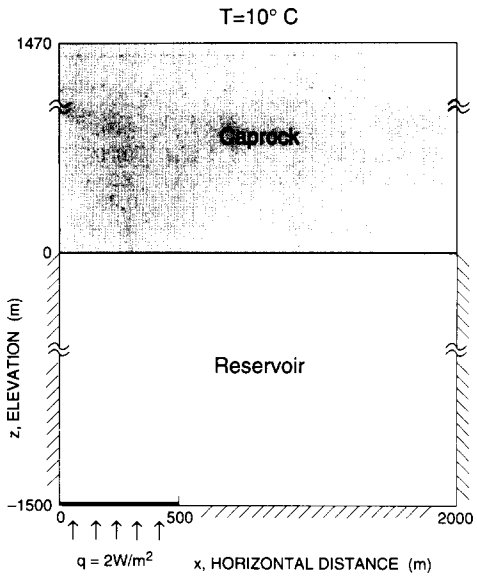

Fig. 1. A schematic representation of the physical problem studied.

caprock maintained at a constant temperature of 10°C at the top representing the ground surface. Heat transfer in the caprock occurs only by conduction.

To investigate mass and heat transport processes involved in the system, the numerical simulator TOUGH2 (Pruess, 1990 and 1991) for simulation of flow of multicomponent, multiphase fluids in geologic media was used. The numerical scheme employed in the code is based on an integral finite difference method (Edwards, 1972; Narasimhan and Witherspoon, 1976). In the present study, uniform mesh sizes are used for both x and z directions with a grid spacing of 100 m, resulting in a 20 × 15 grid. Brief sensitivity studies on the grid size showed that this spacing is sufficiently fine to illustrate flow and heat transfer processes occurring in the system.

The conductive heat loss through the caprock was considered semi-analytically using the method of Vinsome and Westerveld (1980). The temperature of vapor-dominated geothermal reservoirs is typically around 240°C, and this is the temperature we wanted near the top of the reservoir. This was achieved by choosing a caprock thermal conductivity of 3.2 W/m°C and thickness of approximately 1470 m, resulting in an average temperature of 240°C at the reservoir top in order to conduct all of the injected heat to the ground surface.

The phase distribution at steady state depends strongly on the assumed mass of fluid in place (i.e. steam saturation). To test this hypothesis, numerical studies were performed to examine the effects of steam saturations on the phase and behavior of flow and heat transfer processes under steady-state conditions. In the numerical simulations, four cases with different uniform initial steam saturations of 25, 50, 70, and 75% (Cases 1–4, respectively) and with a "high" permeability of 1×10^{-13} m^2 were designed to investigate the basic temperature, pressure, and phase distribution of the two-phase geothermal reservoirs. Cases 5 and 6 investigate the effects of lower reservoir permeabilities, and Case 7 examines the results using a "high" capillary pressure function.

The parameters held constant in all of the simulations performed in the study are given in Table 1. These values are considered to be appropriate for The Geysers and Larderello. A linear relative permeability function is assumed with residual liquid and vapor saturations of 25% and

Table 1. Formation parameters held constant in the simulations

Parameter	Value
Density (kg/m^3)	2650
Specific heat (J/kg°C)	1000
Heat conductivity (W/m°C)	3.2
Porosity	0.03
Relative permeability:	$S_{rw} = 0.25$
(Linear function)	$S_{rg} = 0.05$

Table 2. Reservoir parameters used for the different simulations

Case no.	Permeability (m^2)	Maximum capillary pressure (bar)	Initial steam saturation (%)
1	1×10^{-13}	0	25
2	1×10^{-13}	0	50
3	1×10^{-13}	0	70
4	1×10^{-13}	0	75
5	1×10^{-14}	0	25
6	1×10^{-15}	0	25
7	1×10^{-15}	100	25

5%, respectively. Table 2 shows physical parameters that were varied in the different simulations. As mentioned above, the simulations are run to steady state, where temperature and pressure are constant to within a fraction of a degree and a few pascals. It is acknowledged that in actuality most geothermal reservoirs are not in a steady state but in a quasi-steady thermodynamic equilibrium. This equilibrium has probably been established in a time frame of hundreds or thousands of years, and we have found it takes thousands of years of simulation time to reach steady state in our numerical experiments. The differences in the distribution of temperature, pressure and vapor saturation from an evolution time of hundreds of years compared to thousands of years is not very large.

SIMULATION RESULTS

Base case—25% initial steam saturation

As a base case we consider a uniform initial steam saturation of 25% and a relatively high reservoir permeability of 1×10^{-13} m^2, but neglect capillary pressure (Case 1). In this case, a large amount of mobile liquid is present in the system. The liquid tends to drain to the lower portion of the reservoir and the vapor to rise to the upper portion because of the large density difference between liquid and vapor. As a result, phase segregation occurs in the system. Figure 2a shows the steam saturation and mass flux distributions, with the mass flux representing the summation of the mass flux in liquid and steam phases. Two distinct zones with different steam saturations develop in the reservoir. In the upper two-phase vapor-dominated zone ($z > -500$ m), counterflow with an equal mass flux of steam (up) and liquid water (down) (i.e. a heat pipe) develops; the mass flux in the two-phase zone is small and negligible compared to that in the underlying liquid zone ($z < -500$ m). The behavior of steam–water counterflow and heat transfer in heat pipe was investigated by Martin *et al.* (1976). When the two-phase vapor-dominated zone develops, the vertical pressure gradient is slightly larger than that of a vapor-static column as steam is allowed to flow upward. In addition, the liquid saturation must be low

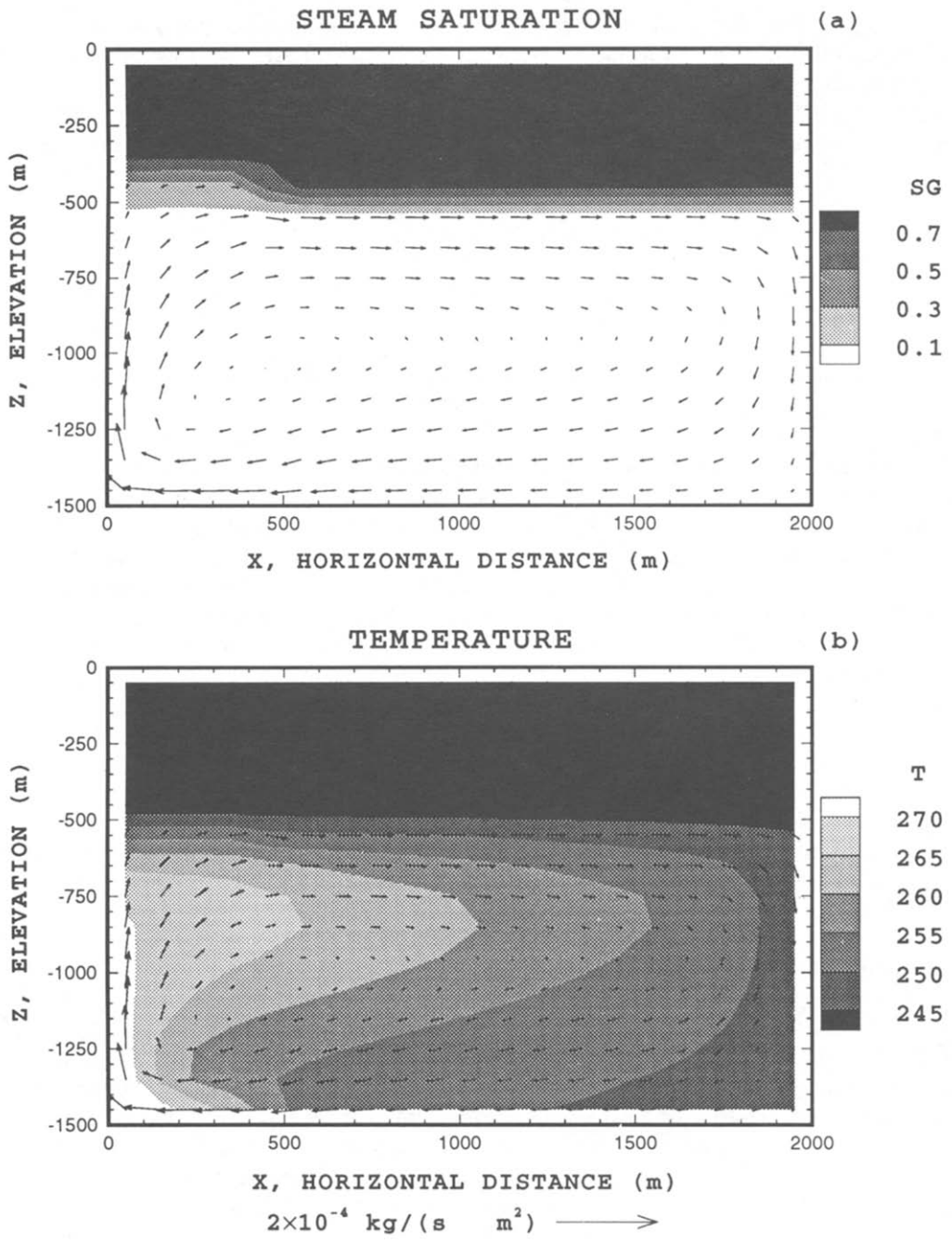

Fig. 2. Case 1 (initial steam saturation 25% and permeability 1×10^{-13} m^2). Steady-state distribution in the reservoir of (a) steam saturation and (b) temperature. Arrows indicate mass flux; their length is proportional to flux magnitude.

so that relative permeability for liquid water is small. Thus only a small amount of liquid water is mobile in the system. Because the irreducible liquid saturation used in simulations is 25%, steam saturation in the two-phase vapor-dominated zone is approximately 75%. The heat pipe effectively transports large amounts of heat for a very small vertical temperature gradient. The

results suggest also that with these conditions a two-phase liquid–vapor reservoir with a localized heat flux from below results in a gravitationally stable system with a vapor-dominated two-phase zone overlying a liquid zone.

Figure 2b shows the temperature and mass flux distributions in the reservoir. The heat transfer in the liquid zone occurs by both conduction and convection, but primarily by convection. The adiabatic boundary conditions and the constant heat flux imposed at the bottom on the left-hand side of the system serve to induce and sustain a buoyancy-driven flow. The recirculatory flow field observed in the liquid zone is a direct consequence of the buoyancy forces induced near the heat source. As a result of the unicellular convective flow developed in the entire liquid zone, the high-temperature isotherm formed near the left bottom portion of the heat source was carried to the upper surface of the zone and laterally to the right end of the zone, while the low-temperature isotherm developed near the upper right portion of the zone was carried to the lower surface and then laterally to the left portion of the zone. This results in a highly stratified region near $z = -560$ m and $0 < x < 500$ m where a sharp temperature gradient is formed.

As expected, the highest temperature of approximately 275°C is found in the bottom of the left wall (near the heating surface), and as a result liquid viscosity and density are lower there. The combined effects of the lower liquid viscosity and density enhance the convective water flow, and thus mass flux in the bottom left corner. Consequently, the liquid returning from the unheated region is observed to flow at a higher velocity toward the heated region, especially in a region near the bottom surface, resulting in a cold liquid intrusion zone immediately above the heat source. The inflow of cooler water causes a temperature reversal in the temperature gradient around the edge of the heated zone ($x = 450$ m) as shown in Fig. 3a. The temperature profile close to the upflow zone ($x = 50$ m) shows interesting but common characteristics. This profile, in conjunction with the pressure profile (Fig. 3b), could be interpreted to yield a vapor-dominated two-phase shallow zone (above −450 m elevation), a liquid-dominated two-phase zone below that (−450 to −800 m elevation) and perhaps an internal flow between −800 and −1400 m elevation in wells open at these depths. However, our results show that the temperature profile observed from −450 to −800 m elevation is due to a liquid-phase convection as opposed to liquid-dominated two-phase conditions. The temperature profile at $x = 1950$ m shows a typical convection type isothermal temperature profile below the vapor zone. However, we are not aware of any field data that show an isothermal 245°C temperature below a 235°C vapor-dominated zone.

Effect of initial steam saturation

In this section the results of the base case (25% saturation) are compared to other cases with higher vapor saturation. As the initial steam saturation increases to 50% (Case 2), the mass of fluid in place is decreased and the amount of mobile liquid water is reduced. Figures 4a and 4b show the distribution of phase saturation and temperature and flow vectors at steady state for this case. The interface between the liquid and two-phase zone is located at a depth of approximately 1050 m; the thickness of the liquid zone is 450 m. Because the aspect ratio of the liquid zone (width over thickness) is larger than that found in Case 1, the effectiveness of convection is decreased, with the convection cell extending over only the left half of the zone. Consequently, the lateral extent of thermal convection is reduced and the heat transfer rates are decreased. This results in relatively high temperatures of approximately 280°C at the left bottom. Thus, in this case a significant portion of the heat in the liquid zone is transported by conduction. However, the temperature in the two-phase vapor-dominated zone still remains at approximately 240°C, in order to provide the proper temperature gradient for conduction heat transfer through the caprock.

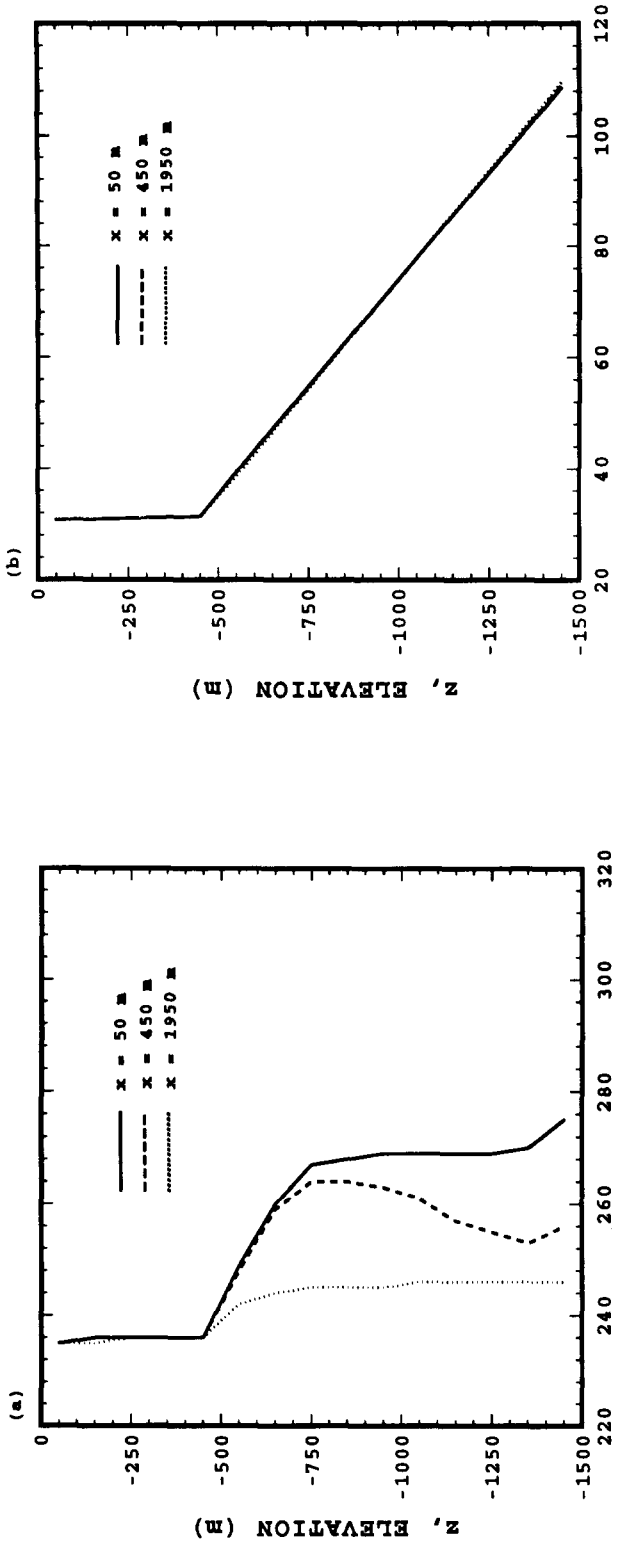

Fig. 3. Case 1 (initial steam saturation 25% and permeability 1×10^{-13} m^2). Steady-state vertical distribution in the reservoir of (a) temperature and (b) pressure measured along different sections.

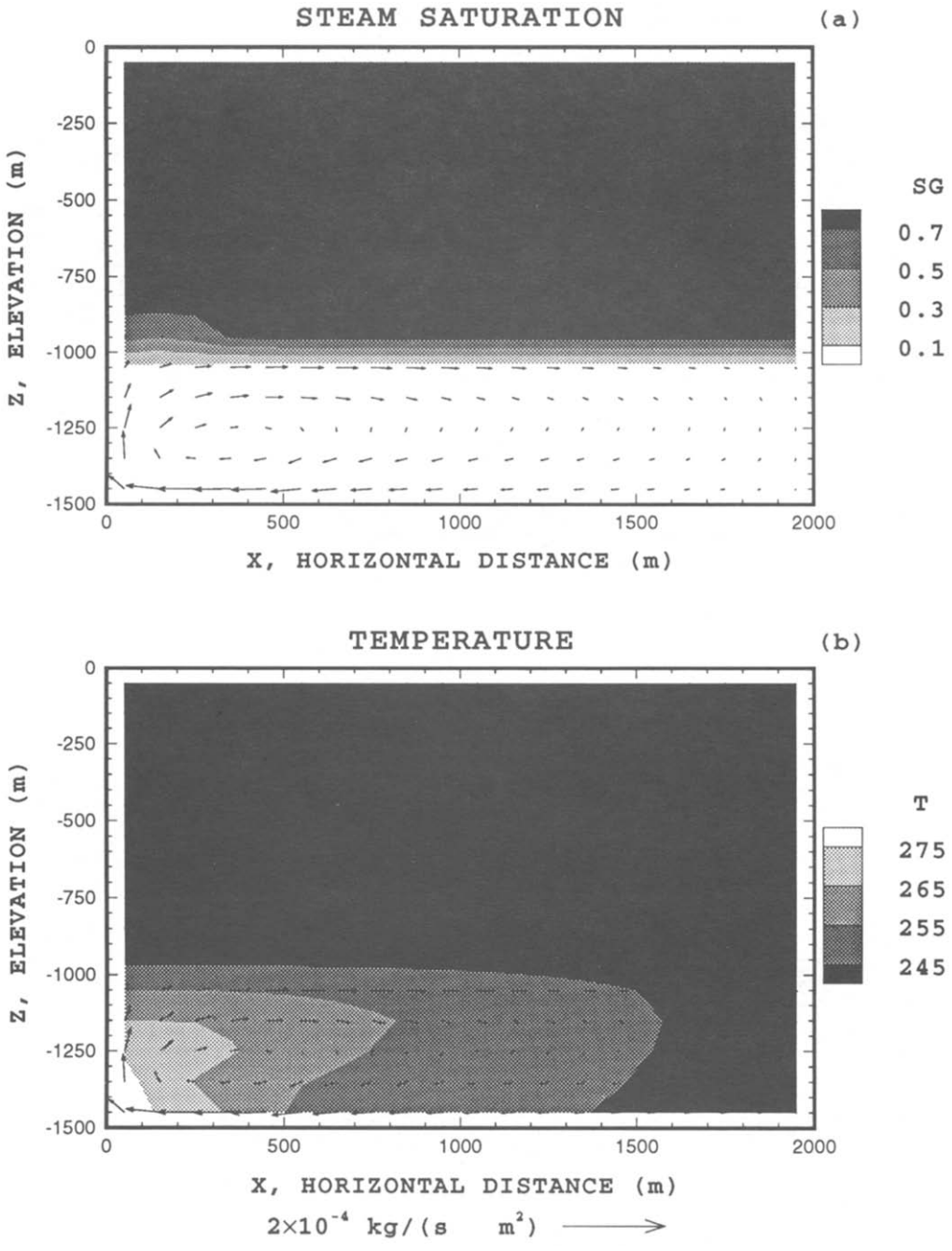

Fig. 4. Case 2 (initial steam saturation 50% and permeability 1×10^{-13} m^2). Steady-state distribution in the reservoir of (a) steam saturation and (b) temperature. Arrows indicate mass flux; their length is proportional to flux magnitude.

When the uniform initial steam saturation is increased to 70% (Case 3), a balanced liquid–vapor counterflow prevails in the entire reservoir, as shown in Figs 5a and 5b. The small temperature variation of 240 to 245°C observed in the system shows the efficiency of the heat pipe in dissipating the heat released from the source. However, when the steam saturation is

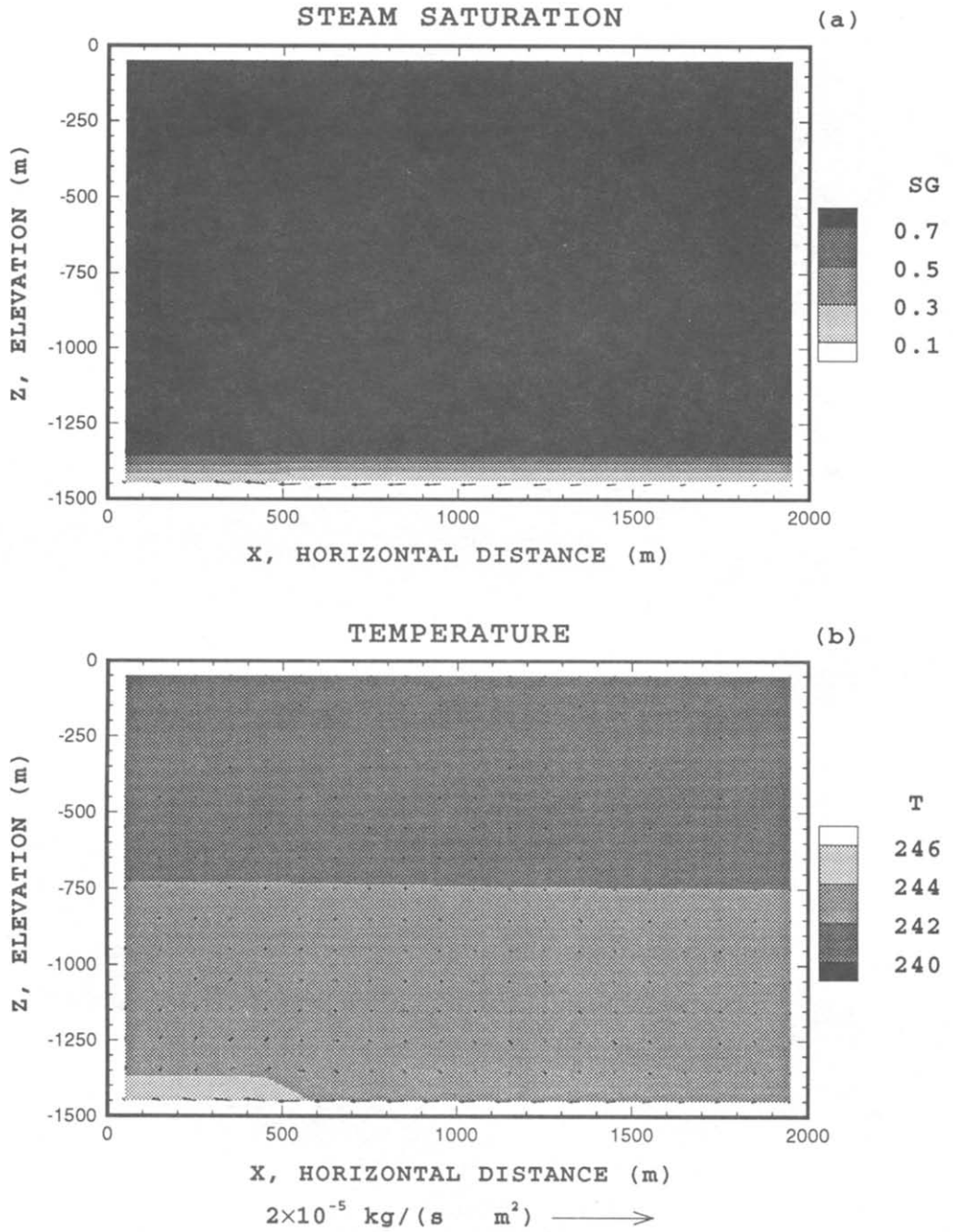

Fig. 5. Case 3 (initial steam saturation 70% and permeability 1×10^{-13} m^2). Steady-state distribution in the reservoir of (a) steam saturation and (b) temperature. Arrows indicate mass flux; their length is proportional to flux magnitude.

increased to 75% (Case 4), the amount of mobile liquid is further decreased and is not sufficient to produce a balanced liquid–vapor counterflow everywhere in the system. Figures 6a and 6b show the distribution of phase saturation and temperature and mass flux for this case. A conduction-dominated zone develops in a region near the heat source. Although a vapor

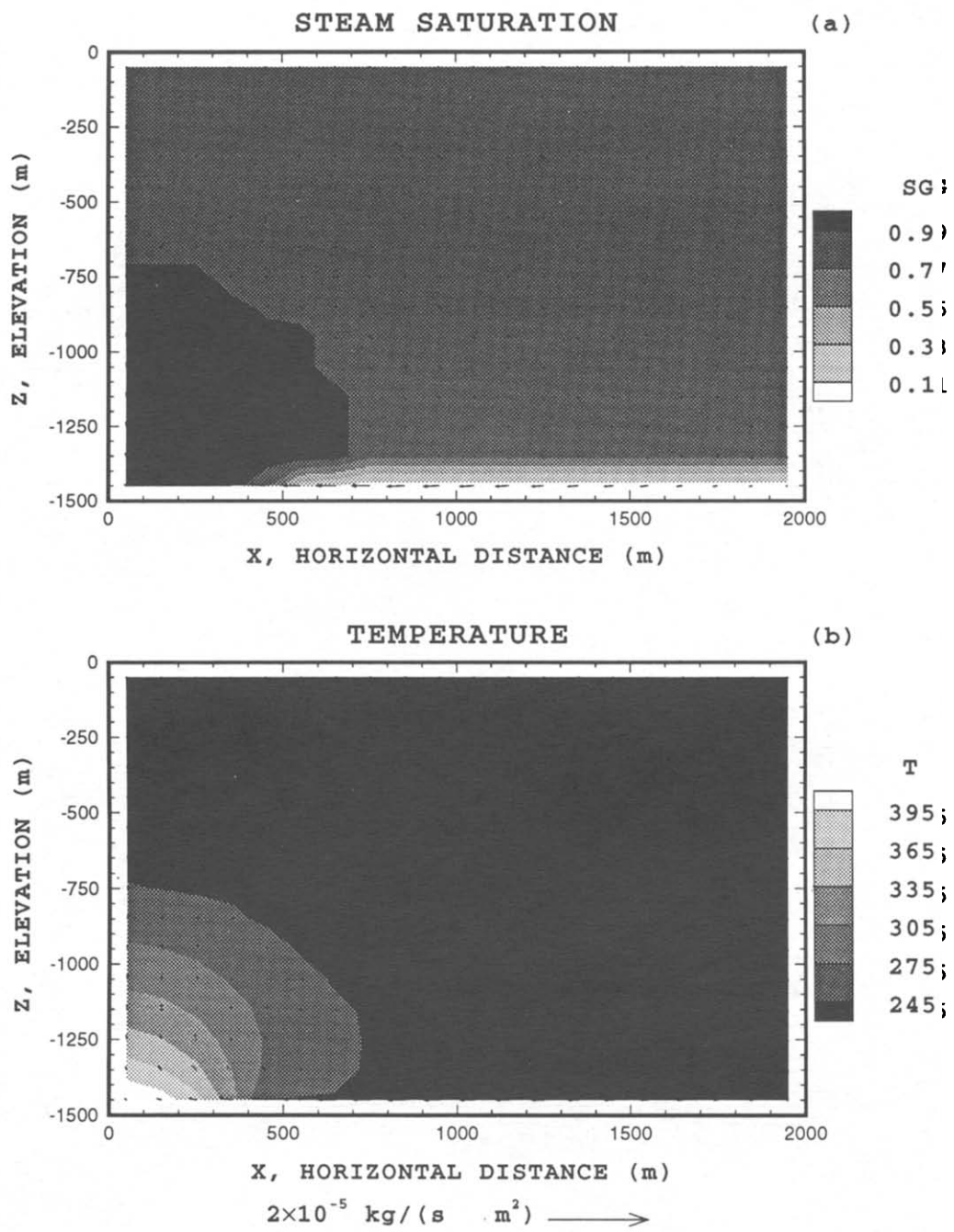

Fig. 6. Case 4 (initial steam saturation 75% and permeability 1×10^{-13} m^2). Steady-state distribution in the reservoir of (a) steam saturation and (b) temperature. Arrows indicate mass flux; their length is proportional to flux magnitude.

convective flow field is observed, it is not nearly as efficient as liquid convective flow in heat dissipation because of the low density of water vapor. Thus, a superheated steam zone develops in the region near the heat source. This may reflect the situation where a superheated vapor zone underlies a two-phase zone observed in the northern Geysers. Figures 7a and 7b show calculated

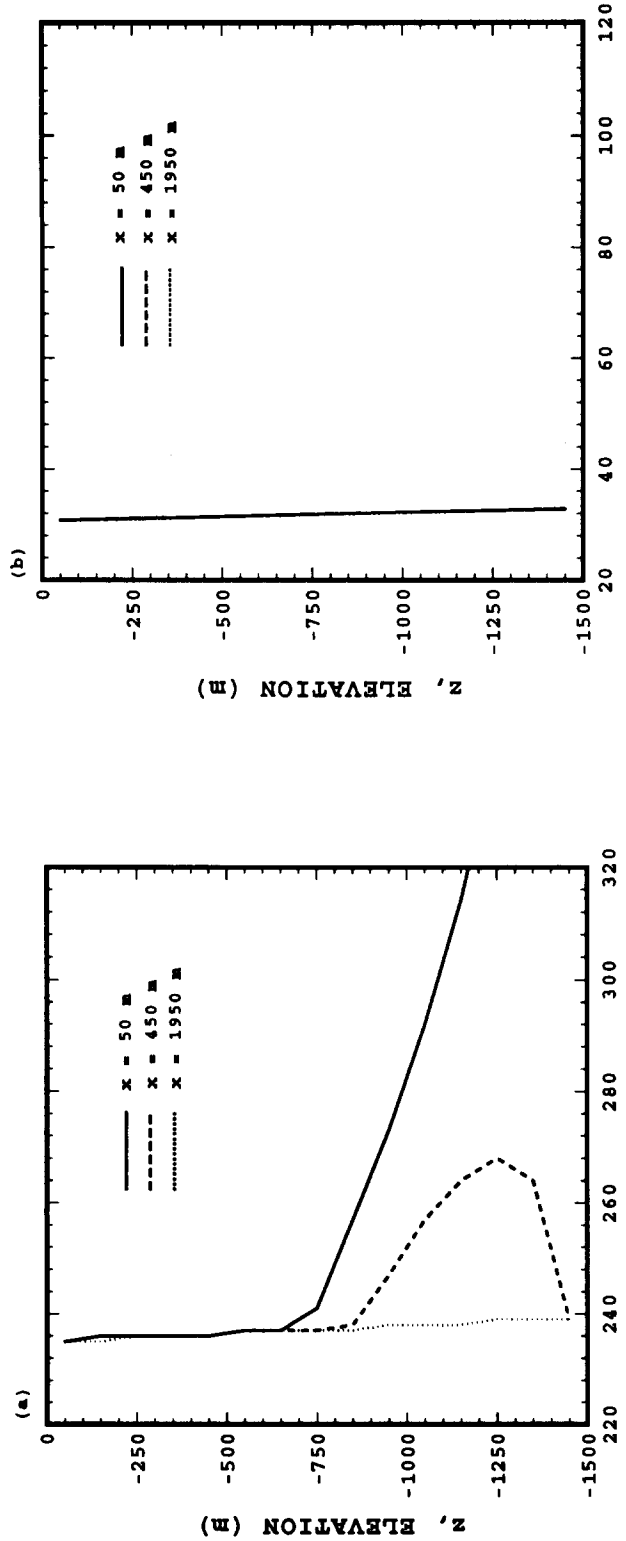

Fig. 7. Case 4 (initial steam saturation 75% and permeability 1×10^{-13} m^2). Steady-state vertical distribution in the reservoir of (a) temperature and (b) pressure measured along different sections.

temperature and pressure profiles at various distances from the symmetry axis ($x = 0$). The figures clearly illustrate the large temperature gradient with a vapor-static pressure gradient below the "typical" vapor-dominated zone, as has been observed at The Geysers (Drenick, 1986; Walters *et al.*, 1988). Figure 7a shows also an apparent temperature reversal at the edge of the heat flux region ($x = 450$ m), which may be an artifact of our numerical grid.

Effect of permeability

To investigate the effects of permeability on flow and heat transfer processes, simulations are carried out with permeabilities of 1×10^{-14} m^2 (Case 5) and 1×10^{-15} m^2 (Case 6). An initial steam saturation of 25% is considered, with the rest of the physical parameters remaining the same as those used in Case 1.

Figures 8a and 8b show the steady-state distribution of phase saturation and temperature and mass flux in the reservoir for Case 5 with permeability of 1×10^{-14} m^2. In general, the flow and heat transfer processes predicted in this case are similar to those found in Case 1, although the lateral extent of strong recirculation is decreased significantly. As the convective heat transfer is weaker, the heat generated by the heat source can not be dissipated as efficiently. This results in development of high temperatures (approximately 310°C) in a region immediately above the heat source, and boiling occurs in the left upper areas of the liquid zone.

When the permeability is further reduced to 1×10^{-15} m^2 (Case 6), a boiling liquid-dominated zone develops in the region above the heat source, as shown in Figs 9a and 9b. Boiling serves to enhance the rate of heat transfer in the region near the heat source. Figures 10a and 10b show calculated temperature and pressure profiles at various locations in the system ($x = 50$, 450, and 1950 m). The temperature profiles above the heated region ($x < 500$ m) indicate a vapor-dominated two-phase zone. This type of profile is observed at several geothermal fields including East Olkaria, Kenya, where permeabilities are similar to those used in the present modeling (Bodvarsson *et al.*, 1987). Close to the right boundary of the model ($x = 1950$ m) the vapor-dominated two-phase zone is underlain by a rather cool single-phase liquid zone. Note that there is a very significant temperature and pressure difference within the vapor-dominated two-phase zone from $x = 0$ to $x = 1950$ m of about 20°C and 10 bars, respectively. The in-place vapor saturation is, however, uniform at about the residual liquid saturation ($S_g = 75\%$).

Effect of capillary pressure

A simulation was carried out to characterize the capillary pressure effect on phase saturation, temperature and fluid flow characteristics. Because capillary pressure functions are poorly known for geothermal systems, a linear capillary pressure function $P_c = P_{max} S_g$ was assumed in the simulations; P_{max} and S_g denote the maximum capillary pressure and steam saturation, respectively. A rather strong capillary pressure function $P_{max} = 100$ bars was used. The rest of physical parameters are the same as those in Case 6 (25% steam saturation and a permeability of 1×10^{-15} m^2).

As expected, when capillary pressure is considered in the calculations, a smoother saturation distribution in the system is obtained. Figures 11a and 11b show the results derived from Case 7, incorporating the capillary pressure effect of $P_{max} = 100$ bars. Because capillary pressure tends to pull water into relatively dry regions, the steam saturation in the upper two-phase zone decreases from 75% to 60%, and the boiling zone immediately above the heat source becomes much wider. In addition, the temperature in the region near the heat source is lower compared to that derived from the case without considering capillary pressure effect. Overall, however, comparison of Figs 11a and 11b with Figs 9a and 9b shows that the capillary pressure effects are not large, even with a relatively strong capillary pressure function.

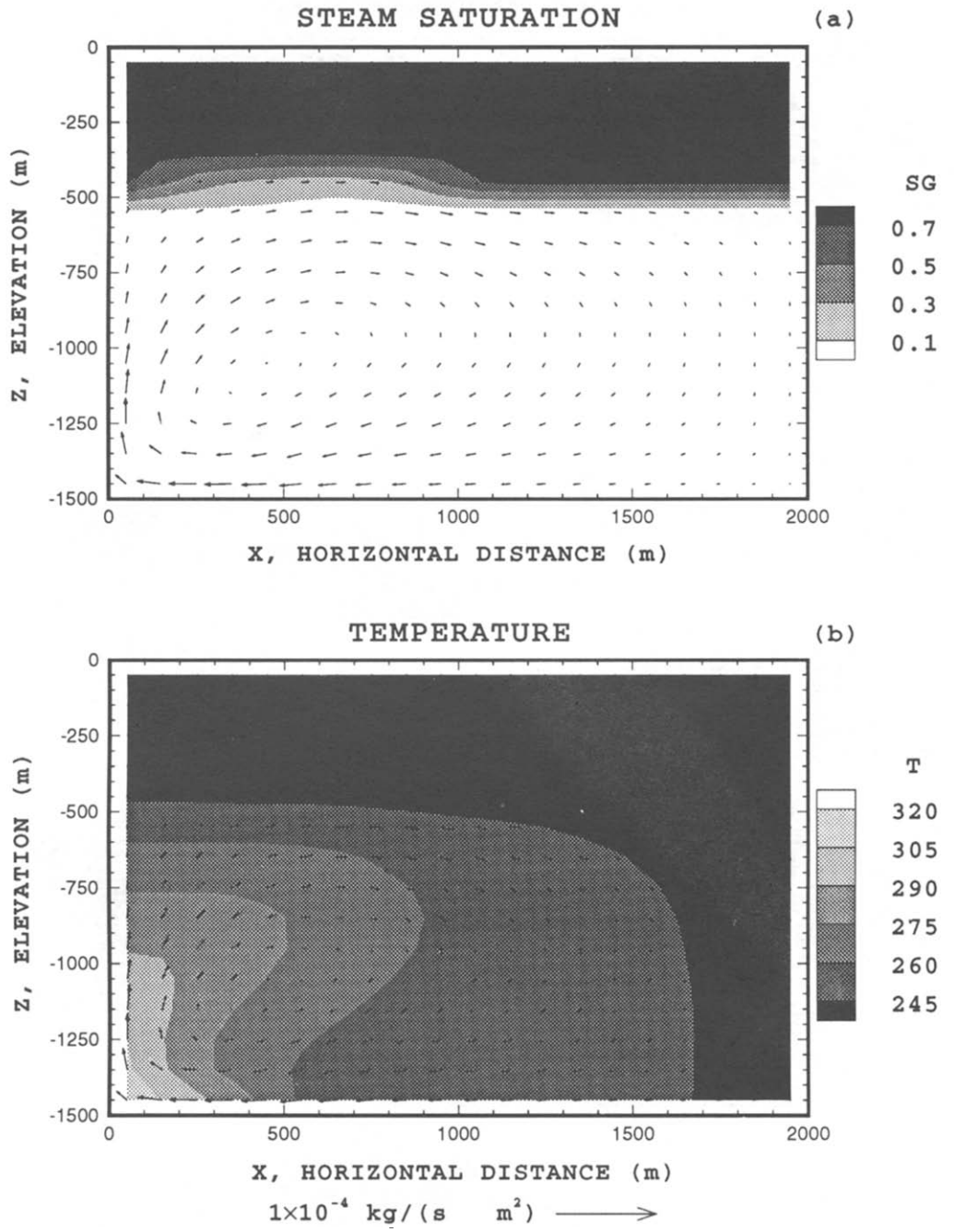

Fig. 8. Case 5 (initial steam saturation 25% and permeability 1×10^{-14} m^2). Steady-state distribution in the reservoir of (a) steam saturation and (b) temperature. Arrows indicate mass flux; their length is proportional to flux magnitude.

CONCLUSIONS

A numerical study of steady-state flow, phase distribution, and heat transfer processes in two-phase geothermal reservoirs was conducted. A two-dimensional porous slab with a localized

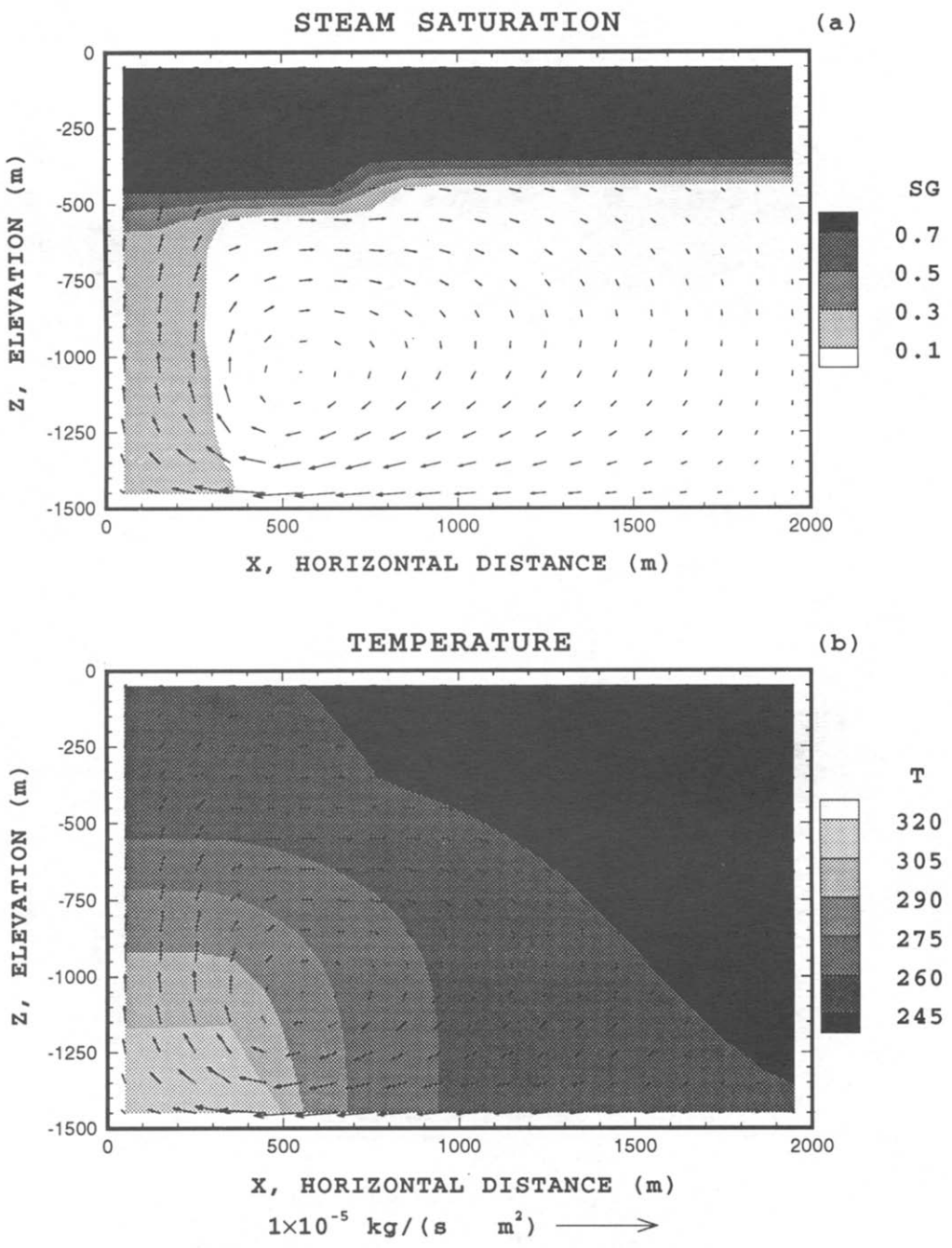

Fig. 9. Case 6 (initial steam saturation 25% and permeability 1×10^{-15} m^2). Steady-state distribution in the reservoir of (a) steam saturation and (b) temperature. Arrows indicate mass flux; their length is proportional to flux magnitude.

heat flux from below was used as an idealized model for a geothermal system. Effects of the mass of fluid in-place (i.e. steam saturation), permeability, and capillary pressure on the phase structure and heat transfer processes were analyzed.

The results show that when a steam saturation of 25% and a rather high permeability of

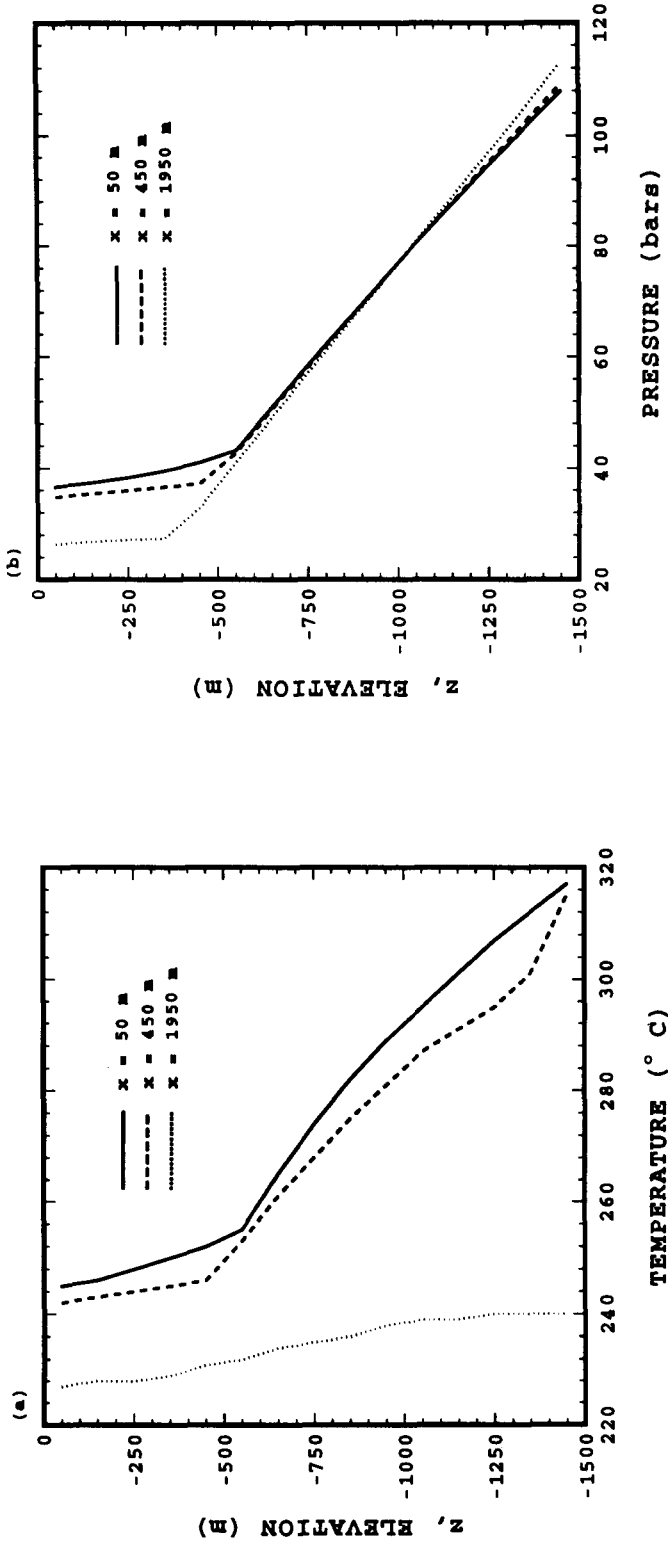

Fig. 10. Case 6 (initial steam saturation 25% and permeability 1×10^{-15} m^2). Steady-state vertical distribution in the reservoir of (a) temperature and (b) pressure measured along different sections.

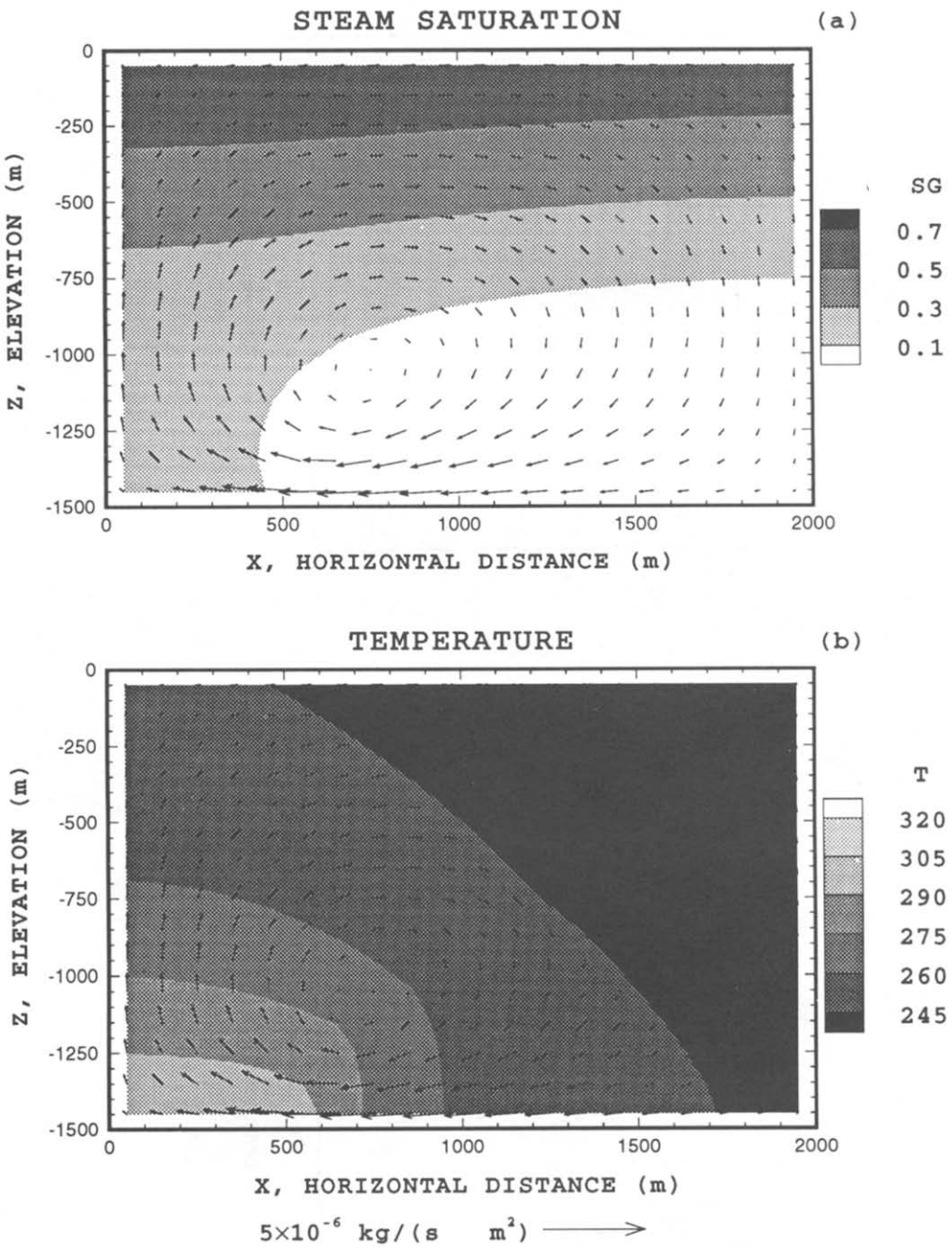

Fig. 11. Case 7 (initial steam saturation 25%, permeability 1×10^{-15} m^2, and maximum capillary pressure $P_{max} = 100$ bars). Steady-state distribution in the reservoir of (a) steam saturation and (b) temperature. Arrows indicate mass flux; their length is proportional to flux magnitude.

1×10^{-13} m^2 are employed, a two-phase vapor-dominated zone overlying a single-phase liquid zone is observed. In the two-phase zone, a balanced liquid–vapor counterflow develops. The vapor rises up to the reservoir top where it is condensed to liquid by releasing the latent heat transferred to the caprock by conduction. The condensate trickles down to the liquid zone. In

the liquid zone, a convective flow field extends laterally over the entire reservoir. However, if the length of heat source varies, the flow characteristics in the liquid zone may be different from that observed in this study.

The strength of the convective flow strongly depends on mass of fluid in place and the permeability of the reservoir. With an increase in steam saturation from 25 to 50%, the convective flow field extends only over the left half of the reservoir, resulting in lower heat transfer rates. As the steam saturation is increased to 70%, a vapor-dominated heat pipe prevails in the entire system. Because a heat pipe efficiently dissipates heat generated by the heat source, the temperature variation in the system is very small, ranging from 240 to 245°C. However, when the steam saturation is further increased to 75%, the amount of mobile liquid is reduced and the heat pipe does not form in the entire system. Under such a circumstance, although a vapor convective flow develops, it is not as efficient as liquid convective flow in dissipating heat, resulting in a high-temperature superheated vapor region underlying the two-phase vapor-dominated zone. Such a high-temperature zone has been found at The Geysers and at Larderello, Italy.

In general, the smaller the permeability considered in the model, the smaller the portion of the liquid zone affected by convective flow, leading to a reduction in heat transfer rates. When a low permeability of 1×10^{-15} m^2 with an initial steam saturation of 25% is used, a two-phase liquid-dominated zone develops, which is consistent with field data from several geothermal fields including Olkaria, Kenya.

To investigate the effects of capillary pressure on features of two-phase geothermal reservoirs, a simulation considering a large capillary pressure was carried out assuming a steam saturation of 25% and a permeability of 1×10^{-15} m^2. The results show that when a large capillary pressure is considered in the model, lower steam saturation is found in the upper two-phase zone, and a wider boiling zone is obtained in the vicinity of the heat source. In addition, the temperatures in the region near the heat source are much lower, because capillary pressure pulls liquid water into a relatively dry and high-temperature zone above the source.

Acknowledgements—The authors thank K. Karasaki and C. Oldenburg for critical review of this paper and valuable suggestions. We appreciate P. Fuller for development of post-processors to visualize simulation results and G. Chen for processing simulation results. This work was supported by the Assistant Secretary for Energy Efficiency and Renewable Energy, Geothermal Division of the U.S. Department of Energy, under contract No. DE-AC03-76SF00098.

REFERENCES

Bau, H. H. and Torrance, K. E. (1982) Boiling in low permeability porous materials. *Int. J. Heat Mass Transfer* **25**, 45–55.

Bodvarsson, G. S., Pruess, K., Stefansson, V., Bjornsson, S. and Ojiambo, S. B. (1987) East Olkaria geothermal field, Kenya. 1. History match with production and pressure decline data. *J. geophys. Res.* **92**, 521–539.

Calore, C., Celati, R., D'Amore, F., Squarci, P. and Truesdell, A. H. (1980) A geologic, hydrologic and geochemical model of the Serrazzano zone of the Larderello geothermal field. *Proc. 6th Workshop on Geothermal Reservoir Engineering*, Stanford University, California, pp. 21–27.

Cappetti, G., Celati, R., Cigni, U., Squarci, P., Stefani, G. and Taffi, L. (1985) Development of deep exploration in the geothermal areas of Tuscany, Italy. *International Volume, Geotherm. Res. Counc.*, pp. 303–309.

D'Amore, F. and Truesdell, A. H. (1979) Models for steam chemistry at Larderello and The Geysers. *Proc. 5th Workshop Geothermal Reservoir Engineering*, Stanford University, California, pp. 283–297.

Drenick, A. (1986) Pressure–temperature–spinner survey in a well at The Geysers. *Proc. 11th Workshop on Geothermal Reservoir Engineering*, Stanford University, California, pp. 197–205.

Edwards, A. L. (1972) TRUMP: A computer program for transient and steady state temperature distributions in multidimensional systems. Lawrence Livermore Laboratory report UCRL-14754, Rev. 3, 259 pp.

Enedy, S., Grande, M. and Smith, J. L. B. (1990) A case history of steamfield development, reservoir evaluation, and power generation in the southeast Geysers. *Geotherm. Res. Counc. Bull.* **19**, 232–248.

Ingebritsen, S. E. and Sorey, M. L. (1988) Vapor-dominated zones within hydrothermal systems: evolution and natural state. *J. geophys. Res.* **93**, 13635–13655.

Lee, D. O. and Nilson, R. H. (1977) Flow visualization in heat generating porous media. Sandia Report SAND 76-0614, Albuquerque, New Mexico.

Martin, J. C., Wegner, R. E. and Kelsey, F. J. (1976) One-dimensional convective and conductive flow. *Proc. 2nd Workshop on Geothermal Engineering*, Stanford University, California, pp. 251–262.

Narasimhan, T. N. and Witherspoon, P. A. (1976) An integrated finite difference method for analyzing fluid flow in porous media. *Water Resour. Res.* **12**, 57–64.

Pruess, K. (1985) A quantitative model of vapor-dominated geothermal reservoirs as heat pipes in fractured porous rock. *Trans. Geotherm. Resour. Counc.* **9**, II, 353–361.

Pruess, K. (Editor) (1990) Proceedings of the TOUGH workshop, Berkeley, California. September 13–14, Lawrence Berkeley Laboratory, Report LBL-29710, 157 pp.

Pruess, K. (1991) TOUGH2—A general-purpose numerical simulator for multiphase fluid and heat flow. Lawrence Berkeley Laboratory Report LBL-29400, 102 pp.

Pruess, K., Celati, R., Calore, C. and Cappetti, G. (1987) On fluid and heat transfer in deep zones of vapor-dominated geothermal reservoirs. *Proc. 12th Workshop on Geothermal Engineering*, Stanford University, California, pp. 89–96.

Ramesh, P. S. and Torrance, K. E. (1990) Stability of boiling in porous media. *Int. J. Heat Mass Transfer* **33**, 1895–1908.

Schubert, G. and Straus, J. M. (1980) Gravitational stability of water over steam in vapor-dominated geothermal systems. *J. geophys. Res.* **85**, 6505–6512.

Sondergeld, C. H. and Turcotte, D. L. (1977) An experimental study of two-phase convection in a porous medium with application to geological problems. *J. geophys. Res.* **82**, 2045–2053.

Thomas, R. P. (1986) Heat-flow mapping at The Geysers geothermal field. Calif. Division of Oil and Gas, Publication No. TR 37, 56 pp.

Torrance, K. E. (1983) Boiling in porous media. *ASME/JSME Thermal Engng Joint Conf. Proc.* Vol. 2, pp. 593–606.

Truesdell, A. H. (1991) The genesis of vapor-dominated geothermal reservoirs with high temperature zones. *Proc. 16th Workshop on Geothermal Reservoir Engineering*, Stanford University, California, pp. 15–20.

Vinsome, P. K. W. and Westerveld, J. (1980) A simple method for predicting cap and base rock heat losses in thermal reservoir simulators. *J. Can. Petrol. Tech.* July–Sept. pp. 87–90.

Walters, M. and Combs, J. (1989) Heat flow regime in The Geysers–Clear Lake area of northern California, U.S.A. *Geotherm. Resour. Counc. Trans.* **13**, 491–502.

Walters, M. A., Sternfeld, J. R., Haizlip, A. F., Drenick, A. F. and Combs, J. (1988) A vapor-dominated reservoir exceeding 600°F at The Geysers, Sonoma County, California. *Proc. 13th Workshop on Geothermal Reservoir Engineering*, Stanford University, California, pp. 73–81.

White, D. E., Muffler, L. J. P. and Truesdell, A. H. (1971) Vapor-dominated hydrothermal systems compared with hot-water systems. *Econ. Geol.* **66**, 424–457.